Impact of Climate Variability on an East Australian Bay

U. Gräwe[a], J.-O. Wolff[a], J. Ribbe[b]

[a] *ICBM, Physical Oceanography (Theory), University of Oldenburg, Oldenburg, Germany*
[b] *Department of Biological and Physical Sciences, University of Southern Queensland, Toowoomba, Australia*

Abstract

The climate along the subtropical east coast of Australia is changing significantly. Rainfall has decreased by about 50 mm per decade and temperature increased by about 0.1 °C per decade during the last fifty years. These changes are likely to impact upon episodes of hypersalinity and the persistence of inverse circulations, which are often characteristic features of the coastal zone in the subtropics and are controlled by the balance between evaporation, precipitation, and freshwater discharge. In this study, observations and results from a general ocean circulation model are used to investigate how current climate trends have impacted upon the physical characteristics of the Hervey Bay, Australia. During the last two decades, mean precipitation in Hervey Bay deviates by 13 % from the climatology (1941-2000). In the same time, the river discharge is reduced by 23 %. In direct consequence, the frequency of hypersaline and inverse conditions has increased. Moreover, the salinity flux out of the bay has increased and the evaporation induced residual circulation has accelerated. Contrary to the drying trend, the occurrence of severe rainfalls, associated with floods, leads to short-term fluctuations in the salinity. These freshwater discharge events are used to estimate a typical response time for the bay.

Key words: Climate variability, drying trend, inverse circulation, hypersalinity, floods

1. Introduction

In subtropical climates where evaporation is likely to exceed the supply of freshwater from precipitation and river run-off, large coastal bays, estuaries and near shore coastal environments are often characterized by inverse circulations and hypersalinity zones (Largier et al. 1997, Tomczak and Godfrey 2003). An inverse circulation is characterised by sub-surface flow of saline water away from a zone of hypersalinity towards the open ocean. This flow takes place beneath a layer of inflowing oceanic water and leads to salt injections into the ocean (Brink and Shearman 2006), examples for such seas include the European Mediterranean Sea, the Gulf of California, the Persian Gulf, the Red Sea and several Australian estuaries and coastal bays (Lavin et al. 1998, deCastro et al. 2004, Ribbe 2006). Due to high evaporation during summer, the accumulation of salt in the head water of these inverse bays/estuaries and atmospheric cooling in the transition to autumn/winter, these water masses can become gravitationally unstable and form gravity current flows (Nunes Vaz et al. 1990, Ivanov et al. 2004).

In this paper, the impact of climate variability is investigated on such an inverse/hypersaline bay. The research is focused on Hervey Bay, a 4000 km^2 large embayment off the central subtropical east Australian coast. In Australia, where climate is characterised by significant inter-annual variability in rainfall (Murphy and Ribbe 2004), longer lasting trends in annual rainfall have been observed since about 1950 (Shi et al. 2008a). Along the densely populated east coast, annual rainfall has declined by more than 200 mm during the period 1951-2000. This reduction in total rainfall has caused persistent drought conditions in the last two decades. These shifts have been attributed to changes in large scale climate system processes such as the Southern Annular Mode, the Indian Ocean Dipole and the El Niño Southern Oscillation (Shi et al. 2008b). The changes that are linked to a widening of the tropical belt are projected to persist into the future. Inter- and intra-annual local rainfall variability and drying trends are strongly linked to variability in the large-scale Pacific Ocean equatorial atmosphere and ocean circulation system.

Recently observed climate changes suggest a widening of the tropical climate belt over the last few decades that is likely to have a significant impact on subtropical climates (Seidel et al. 2008). It leads to shifts in atmospheric and oceanic circulation pattern that together determine the distribution of rainfall.

Severe weather events and extreme high river runoff led to a major sea grass loss in the region of Hervey Bay and impacted adversely upon the dugong (sea cow) population in the past (Preen, 1995, Campbell and McKenzie, 2004) highlighting the regions vulnerability to extreme physical climatic events. Seagrass recovery was monitored for several years (Campbell and McKenzie, 2004). The subtrop-

Email addresses: graewe@icbm.de (U. Gräwe)

ical waters of Hervey Bay are also a spawning region for temperate pelagic fish (Ward et al. 2003) and support the fishery industry worth several tens of millions of dollars, with aquaculture recently developing into a significant industry. Furthermore recent studies showed how the reduction of river discharge and most likely also precipitation, impacts on the fish production on the East coast of Australia (Staunton-Smith et al. 2004, Growns and James 2005, Meynecke et al. 2006). Their findings indicate a reduction in catch due to a decline in freshwater supply. In extreme cases, a reduction of freshwater can lead to hypersalinisation (Mikhailova and Isupovab 2008) in estuaries or the headwater of gulfs. In combination with severe floods and therefore highly variable salt content, the induced stress on species can influence their growing stage (Labonne et al. 2009).

This study show, how these changes in Australian rainfall (short-term variability and trends) have influenced the hydrodynamics of Hervey Bay over the period from 1990 to 2008 and its implications for water quality and ecological response to inputs from the watershed and from the coastal ocean are discussed. This work is a continuation of ongoing research initiated to understand the hydrodynamics/physics of Hervey Bay (Ribbe 2006, Ribbe et al. 2008, Gräwe et al. 2009).

2. Methods and Data

	Summer	Fall	Winter	Spring	Annual
Evaporation [mm/year]	2580	1824	1308	2217	1980
Precipitation [mm/year]	2100	1068	588	936	1173
River discharge [mm/year]	494	456	173	95	305
Wind speed [m/s]	6.4	6.2	5.6	6.6	6.2
Wind direction [degree]	170	120	48	107	110
Air temperature [°C]	25.1	22.2	16.8	21.9	21.5
EAC [Sv]	18.9	14.8	12.9	17.8	16.2

Table 1: Climatological data (1941-2008) of Hervey Bay (southern hemisphere seasons). The southwards water transport of the EAC is computed along 25°S (1990-2008). 1 Sv (Sverdrup) corresponds to a transport of 10^6 m^3/s.

Hervey Bay (Fig. 1) is a large coastal bay off the subtropical east coast of eastern Australia and is situated at the southern end of the Great Barrier Reef to the south of the geographic definition of the Tropic of Capricorn (23.5 °S). Fraser Island separates the bay to the east from the Pacific Ocean. At the northern tip of Fraser Island, an enormous sand spit is located that extends the separation from the open ocean 30 kilometres further to the north. This sand spit, called Breaksea Spit, has an average depth of 6 m and shows some dominant underwater dune features. Hervey Bay covers an area of about 4000 km^2. Mean depth is 15 m, with depths increasing northward to more than 40 m, where the bay is connected to the open ocean via an approximately 60 km wide gap. A narrow and shallow (< 2 m) channel (Great Sandy Strait) connects the bay

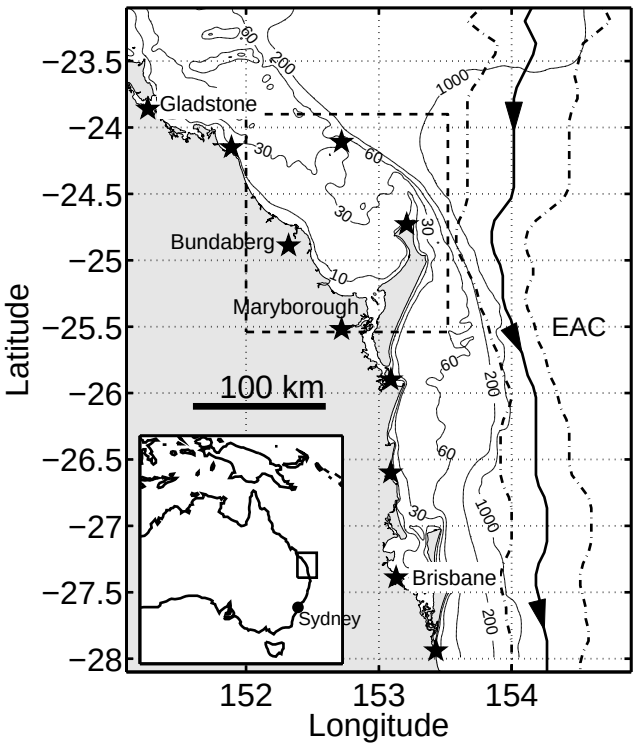

Figure 1: Model domain and location of Hervey Bay. The isolines indicate the depth below mean sea level. The dashed box marks the region of interest and also the location of the inner nested model area (details are given in Fig. 2). The thick black line indicates the mean centre position of the East Australian Current (1990-2008). The dot-dashed lines show the minimum/maximum offshore position of the stream. The location of the weather observation stations are denoted by the stars. Insert: a map of Australia showing the location of the model domain along the east Australian coast.

to the ocean in the south. Two rivers connect the catchments areas with the bay, the Burnett River at Bundaberg and the Mary River at Maryborough. In the east/northeast of Fraser Island, the continental shelf has an average width of about 40 km. At the eastern shelf edge the East Australian Current (EAC) reattaches to the shelf to follow the coastline to the south.

The climate around Hervey Bay is characterised as subtropical with no distinct dry period but with most precipitation occurring during the southern hemisphere summer. The region is influenced by the Trade winds from the east with a northern component in autumn and winter and a southern one in spring and summer (Tab. 1).

2.1. The Model

The numerical computations are performed with the identical model setup as described in Gräwe et al. (2009). For a detailed discussion of the model setup and for validation of the model results the interested reader is referred to their paper. In the following only model details are discussed that are essential to this study.

The hydrodynamic part of the three dimensional primitive equation ocean model COHERENS (COupled Hydrodynamical Ecological model for REgioNal Shelf seas)

(Luyten et al. 1999) is employed in combination with a 2.5 order Mellor-Yamada turbulence closure (Mellor et al. 1982) to achieve vertical mixing. The model domain is resolved using a coarser grid for the outer area and a finer grid for Hervey Bay (one-way nesting). The outer domain (see Fig. 1) is an orthogonal grid of 90×140 points. It covers the region from 151˚-155˚W and 23˚-28˚S. The mesh size varies and increases from 2.5 km within Hervey Bay to 7 km near the boundaries of the model domain. The vertical grid uses 18 sigma levels with a higher resolution towards the sea surface and the bottom boundary. The reason is to accurately resolve the upper mixed layer as well as the bottom boundary layer. The depth within the model domain is limited to 1100 m in order to increase the maximum allowable time step. The inner domain (Fig. 2) has a uniform grid spacing of 1.5 km and a size of 100×120 grid points.

Tidal elevations and phases of the five major tidal con-

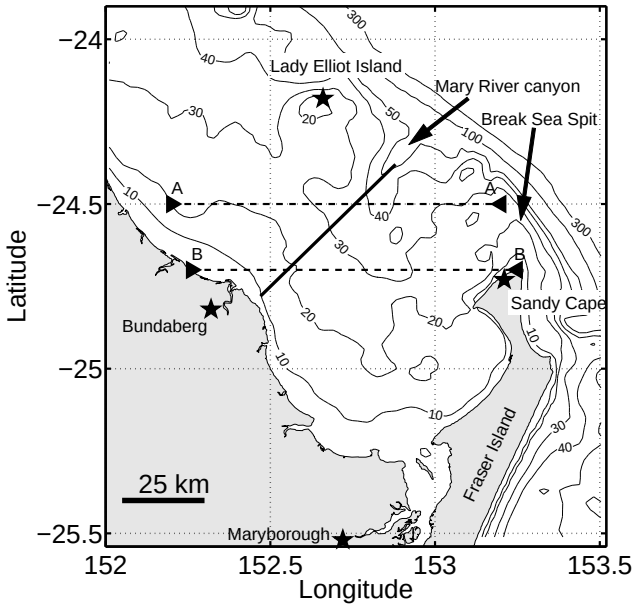

Figure 2: Inner domain and details of Hervey Bay. The isolines indicate the depth below mean sea level. The solid line indicates the position of the salinity/density gradient transect. The dashed line AA is the positions of most northern field trip transect. Location of the weather observation stations are denoted by the stars. The dashed line BB indicates the transect to compute the salinity flux and residual circulation and marks the northern boundary of Hervey Bay.

stituents (M_2, S_2, N_2, K_1 and O_1) are taken from the output of the global tide model/atlas FES2004 (Lyard et al. 2006). Sea surface height, anomalies and the sea surface gradient causing the EAC are prescribed using TOPEX/Poseidon and JASON-1 altimeter data. The lateral open boundary conditions are derived from the global ocean model OCCAM (Ocean Circulation and Climate Advanced Modelling project, Saunders et al. 1999), which has a horizontal resolution of 1/4 ˚and 66 vertical z-levels. To calculate air-sea fluxes (moisture, latent heat, sensible heat, momentum) the COARE 3.0 algorithm (Coupled-Ocean Atmosphere Response Experiment, Fairall et al. 2003) is implemented. The long wave back radiation flux is computed using the formulation of Bignami et al. (1995).

2.2. Data

Hydrographic observations, made during several field trips into the bay (2004, 2007, and 2008) and three-day composite Advanced Very High Resolution Radiometer (AVHRR) sea surface temperature (SST) data from 1999-2005 are utilised to validate the performance of the model. The 2004 field trip, the sampling locations and an analysis of the hydrographical situation within the bay is presented by Ribbe (2006, 2008). To be consistent with the 2004 field trip, the sampling locations for the subsequent cruises (2007 and 2008) were the same.

The model forcing consists of three hourly observations of atmospheric variables (10 m wind (u,v), 2 m air temperature, relative humidity, cloud cover, air pressure and precipitation) of weather stations located along the east coast (see Fig. 1), which were linearly interpolated onto the model domain. The river forcing is taken from daily observations of river discharge gauges (Bureau of Meteorology - BOM, Australia).

In Tab. 1 climatologically data for Hervey Bay are presented. To compare the river discharge with the contributions by precipitation, the fresh water inflow by the Mary River has been converted to a precipitation equivalent (i.e. the thickness of a virtual freshwater layer over Hervey Bay).

For validation of the computed evaporation, time series of measured pan evaporation are used. Available are daily observations for Bundaberg (1997-2008) (BOM). Although the data were quality checked, no information is given for the sampling error. It is known that evaporation from a natural body of water is usually at a lower rate than measured by an evaporation pan. To account for this, a pan correction coefficient is introduced. It can vary from 0.65 (Tanny et al. 2008) up to 0.85 (Masoner et al. 2008). Here a correction factor of 0.75 is chosen.

The climatological volume transport by the EAC (Tab. 1)

	Bundaberg	Sandy Cape	Maryborough	Mary River
1941-1970	1119.8	1172.7	1187.7	294.1
1971-2000	1029.7	1306.9	1221.8	315.9
1941-2000	1074.8	1239.8	1204.8	305.0
variability	45.1 (4%)	67.1 (5%)	7 (1%)	10.9 (4%)
1990-2008	988.7	1052.4	1008.1	235.2
reduction	8%	15%	16%	23%

Table 2: Detailed climatological data of precipitation and river discharge (precipitation equivalent) in mm/yr.

was computed using velocity fields of the OCCAM model. The transect to estimate the southwards transport was placed at 25˚S. The mean transport of 16.2 Sv and the annual variations are in good agreement with the estimates made by Ridgway and Godfrey (1997).

3. Model validation

For model validation, transects of density (Fig. 2 transect A-A)in the northern part of Hervey Bay are shown in Fig. 4. A validation of the distribution of salinity and temperature within the bay for 2004 and 2007 is given in Gräwe et al. (2009). Here the focus is on the most northern transects available. The model captures the two density plumes for the December 2007 field trip (Fig. 4a) at 152.3°E and 152.8°E. The model misses the proper timing of the upwelling event that is visible in the observation. It seems that this event is lagged by two days in the simulations. For the May and June 2008 field trips, the agreement is quite well. The model reproduces the frontal structures and the vertical well-mixed conditions on the shelf.

In order to demonstrate the model performance to capture the dynamics on longer time scales, pan-evaporation data and satellite AVHRR SST data have been used for the model validation. The comparison between the measured and simulated evaporation is shown in Fig. 3a. Due to the expected higher sampling errors in the pan-evaporation measurement, the data scatter is wider than for the SST comparison. R^2 with 0.8 is reasonably high. The linear fit indicates, that the model tends to underestimate high evaporation rates and vice versa overestimates low evaporation rates, but this systematic error is quite small.

Fig. 3b shows the comparison of bay averaged model SST data and AVHRR satellite data. The linear fit indicates that the model reproduces the measurements with a vanishing bias. R^2 with 0.82 is again quite high.

The simulated southward transport of the East Australian Current is on average 7.1 Sv, which is much less than the EACs seasonal average of 16.2 Sv (see Tab. 1). Further, the centre location of the EAC in the simulations is shifted in the northern part of the model domain towards the 1000 m depth contour by 30-40 km. However, given the unrealistic maximum depth of 1100 m, this transport is assumed representative of a baroclinic EAC flow. Oke and Middleton (1999) also used the same argument.

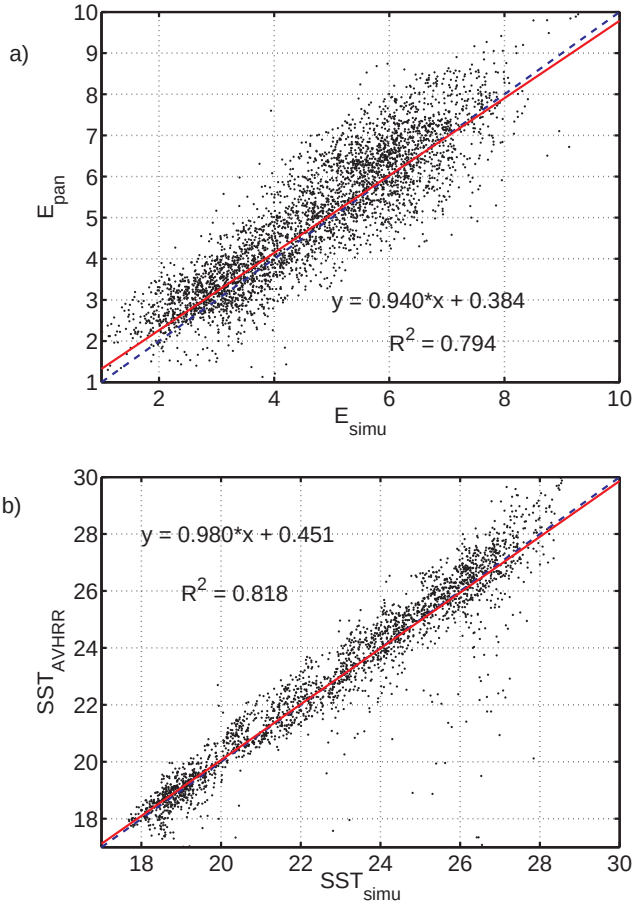

Figure 3: Scatter plot of a) simulated evaporation vs. measured pan evaporation [mm/day] and b) simulated SST vs. AVHRR SST [K]. The red line indicates a linear fit.

4. Impact of freshwater reduction

4.1. Trends in freshwater supply

Tab. 2 shows the climatology of freshwater supply for the three observation stations surrounding Hervey Bay. The deviations from the climatology (1941-2000) between 1941-1970 and 1971-2000 are less than 5%. The reduction in freshwater supply during the last two decades varies between 10-20% and is therefore higher than the long term variability. This is caused by severe droughts and the ongoing drying trend on the east coast of Australia. Despite the general trend, the precipitation gradient between Bundaberg and Sandy Cape remains nearly the same. To show the reduction in freshwater supply in detail, Fig. 5 depicts the deviation of freshwater input into Hervey Bay from the climatology. Shown are the cumulative sum plots of monthly bay averaged precipitation and Mary river discharge. Two major events are visible. During 1992 strong rainfalls and river floods occurred, caused by an El Niño event. The classification into El Niño/La Niña are based on the Oceanic Niño Index (ONI). This was quite unusual, because during El Niño, the Australian east coast normally experiences drought conditions. The floods and rainfalls in 1999-2000 occurred during a strong La Niña event. In 1992, the freshwater supply recovered to the climatology. Although the rainfalls in 1999-2000 were significant, they could not replenish the water deficit. Due to long/persistent droughts, the soil moisture in the catchments were low, thus a certain amount of rainfall was needed first to recharge soil moisture and ground water, until significant runoff could be released. Therefore, the La Niña events 1996 and 2008 show a signature in the river discharge but are in general of minor importance.

In the following, the numerical model is used to quantify, how this reduction of freshwater fluxes affected Hervey Bay.

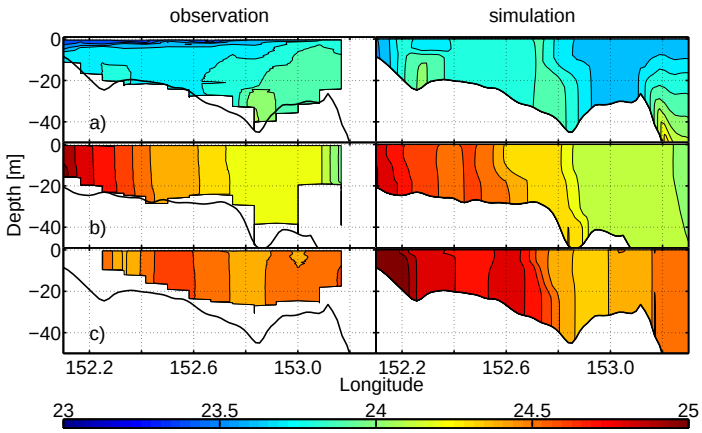

Figure 4: Comparison of density σ_t $[kg/m^3]$ transects; a) along 24.5°S during December 2007, b) along 24.4°S during May 2008 and c) along 24.5°S during June 2008.

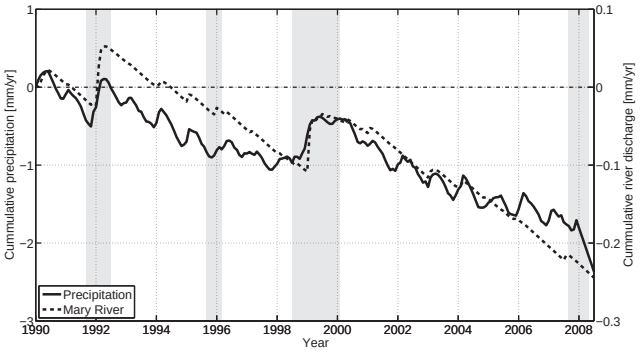

Figure 5: Deviation of freshwater flow into Hervey Bay from the climatology (1941-2000). Shown are the cumulative sum plots of monthly bay averaged precipitation and Mary river discharge. The grey bars indicate El Niño/La Niña events. Note that the river discharge has a different scaling to emphasise details.

4.2. Hypersalinity and inverse state

To define hypersalinity and the inverse state, a transect is placed in Hervey Bay (perpendicular to climatological isolines of density/salinity) along which gradients of density and salinity are computed (see Fig. 2). The thresholds to define hypersalinity $\partial S = 2 \cdot 10^{-3} psu/km$, inverse state $\partial\rho = 0.01 kgm^{-3}\ /km$ are taken from Gräwe et al. (2009). Contrary to their setup the location of the transect is shifted 30 km to the north and is now aligned with the position of the Mary River Canyon. This is motivated to include the discharge of the Burnett River.

The density (Fig. 6a) and salinity (Fig. 6b) gradient times series clearly show the impact of the 1999 and 2008 La Niña and also the 1992 El Niño event. Further during the last decade less frequent reversals of the salinity gradient occurred. To understand the impact of the drying trend, the days in the year are computed, where the salinity gradient and the density gradient exceed the critical thresholds. A year is defined from July to June and therefore the complete southern hemisphere summer is included in one year. The results are shown in Fig. 6c. A linear fit has

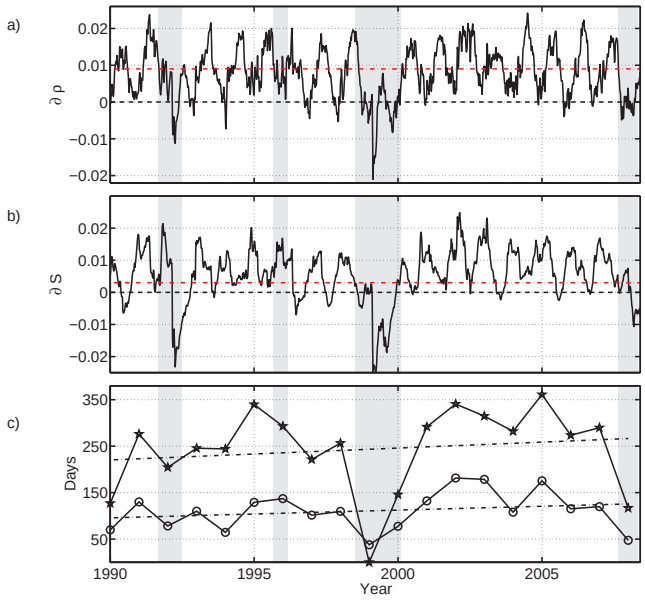

Figure 6: a) Time series of density gradient - $\partial\rho$ $[kg/m^3/km]$, b) salinity gradient - ∂S $[psu/km]$. Shown are daily averages. The red dashed lines indicate the thresholds given in the text and c) depicts the number of days per year where hypersaline/inverse conditions are found. To indicate the trend, linear fits are added. The grey bars show El Niño/La Niña events.

been additionally added to both time series. Hervey Bay is, on average, during 240 days of the year in a hypersaline state and for 108 days in the inverse state, respectively. Interesting to note is that due to the ongoing drying trend, both time series show a rising trend. The model simulations indicate an increase of 2.7 days per year, where Hervey Bay is hypersaline and an increase of 1.8 days per year for inverse conditions. These trends are clearly biased by the El Niño/La Niña events. The 1999 floods and rains lowered the mean but only slightly biased the trend. The 2008 La Niña reduced the trend. Therefore, these trends should be judged with care. If ignoring the 1999 La Niña, the observed trend would be in the range of the inter-annual variations and indicates significance.
The time series indicate that Hervey Bay shows different behaviour before/past the 1999 La Niña event. Before 1999, the bay was on average on 250 days in a hypersaline state. After the 1999 La Niña event this raised to 300 days on average. This switch is caused by the ongoing drought conditions on the east coast of Australia.

4.3. Residual circulations

Due to the water loss by evaporation and the thereby established hypersalinity zone, a baroclinic circulation is induced in Hervey Bay. Gräwe et al. (2009) estimated the average velocity of this clockwise flow in the bay with about 2 cm/s. To understand the impact of the reduced freshwater supply, a time series of this residual flow is given in Fig. 7b. To remove any barotropic influence, a model run was started, where temperature and salinity

were switched off. The induced residual flow was then subtracted from the baroclinic case. The mean flow is on average 2 cm/s. A closer inspection of the time series shows that the flow is weaker during summer than during winter. This seems puzzling but the weakening of the evaporation induced residuals during summer is caused by the EAC. In Tab. 1 the transport of the EAC is given (see also Fig. 1). The current is strongest during summer (18 Sv) and weaker during winter (12 Sv). The EAC induces an anti clockwise circulation within Hervey Bay. This residual flow is estimated to be in the range of 1-2 cm/s and therefore of the same order as the evaporation induced clockwise flow. Thus, during summer the EAC can slow down the evaporation induced flow. Furthermore, this flow shows a rising trend. The increase during the simulation period is about 18%. Fig. 7b also shows the standard deviation, which is in the same range as the estimated trend. Thus, during the two decades of simulations the reduction of freshwater leads to an acceleration of the residual circulation.

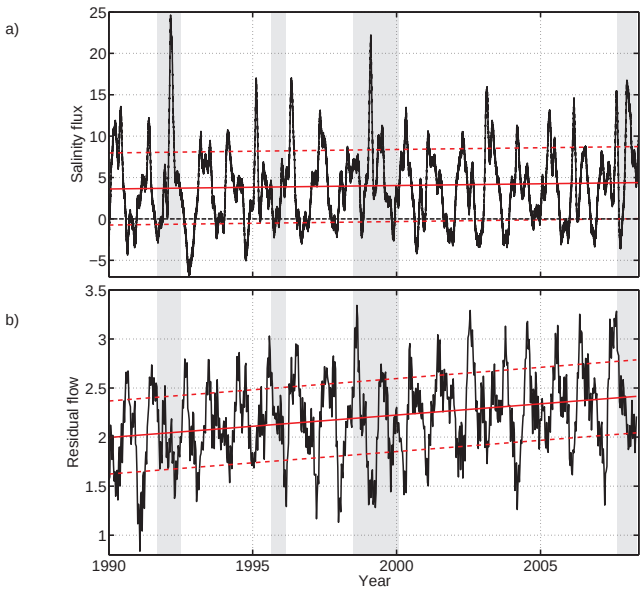

Figure 7: a) Time series of salinity flux (daily averages) - $[ton/s]$ and b) residual circulation (fortnightly averages) - $[cm/s]$. To indicate the trend, linear fits are added. The red dashed lines indicate the standard deviation. The grey bars show El Niño/La Niña events.

4.4. Salinity flux

To quantify the overall residual mass flow, the salinity flux of the bay has been calculated explicitly by computing the transport through advection and diffusion across the open boundaries (Ω) of Hervey Bay.

$$F_{Salt}(t) = \int_{\Omega} v(x,z,t)S(x,z,t) \; + \; K_H(x,z,t)\frac{\partial}{\partial y}S(x,z,t)\; d\Omega \qquad (1)$$

The northern boundary is defined along the dashed line B-B in Fig. 2 and the southern boundary is located in the Great Sandy Strait at 25.5°S. The first term in Eq. 1 represents the flux due to advection (meridional velocity times salinity) whereas the second term represents the diffusive fluxes. K_H is the turbulent scalar horizontal diffusivity (along sigma-coordinates). The model indicates that since 1990, the salinity flux has increased by about 22 % (linear fit in Fig. 7a). This corresponds to a rise of approx. 0.9 ton/s during the simulation period. The mean flux is estimated to be 3.95 ton/s. Again the standard deviation is indicated, which is now with 4.1 ton/s the fourfold on the trend. Thus, the model indicates a trend, but to show that this increase is significant, the simulation period has to be at least doubled.

4.5. Impact of EAC

To quantify the importance of the EAC on the hydrodynamics in Hervey Bay, two additional experiments were conducted. The aim was to reduce the southward transport of the EAC. The average transport is approx. 7.1 Sv. In the first experiment, the transport was reduced to 3.5 Sv and in the second experiment, the EAC was completely switched off. These modifications were incorporated by reducing the background sea surface gradient, causing the EAC. To preserve the dynamics, the sea surface height anomalies were left unchanged.
The comparison of the results with the measurements from the field trips show, that the impacts on the temperature field were of minor importance. The variations in the salinity field were noticeable. The influence of the EAC is visible in the salinity/density gradient time series. The EAC smoothes the salinity and density differences. By completely switching off the EAC, the peak value of the salinity gradient increased by 12 % and for the density gradient by 10 %, respectively. The simulations thus indicate that variations in flow strength of the EAC are noticeable, but of less importance. A possible explanation is that the stream reattaches south of 25°S to the shelf. Further Break Sea Spit (Fig. 2) shields Hervey Bay from the ocean. In conclusion, the EAC has only little influence on Hervey Bay.
Finally, the southward transport was investigated to detect a possible trend in the volume transport. The analysis showed that the EAC slightly accelerates, but the trend in the two decades is less than 1/6 of the standard deviations and thus not significant.

5. Short term variability

The Intergovernmental Panel on Climate Change (IPCC) predicts that heavy precipitation events become more frequent over most regions throughout the 21 st century (IPCC, 2007). This would affect the risk of flash flooding and urban flooding. Australia's strongest examples were in 1973-74 (Brisbane's worst flooding this century in January

1974), 1988-89 (vast areas of inland Australia had record rainfall in March 1989) and May 2009. In this recent example, within some days, approx. 300 mm rains (in total) were measured along the Sunshine Coast (Brisbane up to Hervey Bay). This is around one third of the annual mean. Northern Brisbane had peak values of 330 mm/day. Unfortunately, these data could not be compiled into the simulations. However, Fig. 8 shows times series of the Mary River and Burnett River discharge. Two extreme flooding events are visible, one in February 1992 and in February 1999. The latter led to significant loss of seagrass in the Great Sandy Strait (Campbell and McKenzie, 2004). Because the peak values of the Burnett River are only about one sixth of the maximum flow of the Mary River, the focus of the short-term variability is on the impact of the Mary River.

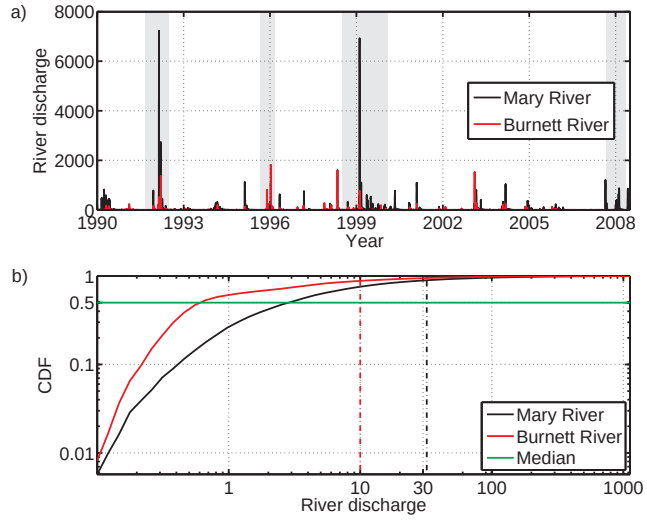

Figure 8: a) Freshwater discharge of the Mary and Burnett River (1990-2008) in m^3/s. The grey bars indicate El Niño/La Niña events and b) Cumulative distribution functions (CDF) of the freshwater discharge (in m^3/s) of the Mary and Burnett River (1990-2008).The two dashed lines indicate the mean

5.1. River discharge statistics

The catchments area of the Mary River covers 5000 km^2. It reaches from 25.2°to 27°S and from 152° to the coast (see Fig. 1), thus a stripe of 150×50 km^2. The Mary River flows into the northern region of the Great Sandy Strait draining a modified catchments of dryland grazing, agricultural crops, cleared land, forests and both sewered and unsewered urban development areas (Rayment and Neil, 1997). For an average rainfall year, 21% of rainfall is exported as runoff into the Mary River and 268,000 tonnes of eroded sediments flow into near shore regions annually. The river further flushes nitrogen (1.7 kg/ha/y) and phosphorus (0.2 kg/ha/y) into the Great Sandy Strait passage each year (Schaffelke, 2002).

The river discharge time series in Fig. 8a are rather spiky. The peak values for the 1992 and 1999 flood reached 7000 m^3/s. In Fig. 8b the cumulative distribution functions (CDF) for the Mary and Burnett Rivers are given. The mean flow for the Mary River is 30 m^3/s and 10 m^3/s for the Burnett River. The Median is 3 m^3/s and 0.8 m^3/s, respectively, and therefore only a tenth of the mean. Thus, most of the time both rivers are almost dry. The rare extreme events shift the mean to higher values. The CDF indicates, that the probability to exceed a flow rate of 70 m^3/s for the Mary river and 30 m^3/s for the Burnett River is less than 5%. Fig. 8a further indicate that the high flow volumes are strongly linked to El Niño/La Niña events.

5.2. Flooding events

In Fig. 9 the response of Hervey Bay to flooding events is shown. Plotted are the depth averaged salinity field and a transect in the southern part of the bay, 10 days past the peak flow of the Mary River. The river discharge associated with these flooding events is 7100 m^3/s (1992), 6700 m^3/s (1999) and 900 m^3/s (2008), see also Tab. 3. The peak value of 900 m^3/s seems rather low, compared to the 1992 event. However, the 2008 flood was preconditioned by three 750 m^3/s peaks (in the 40 days before the flood) and puts it therefore in a comparable range to the 1992 event. Fig. 9 indicates that the outflow of the freshwater is restricted to a narrow region along the western coast. The transects for 1992 and 1999 further indicate a pronounced frontal structure (horizontal and vertical). Beside this narrow coastal freshwater strip, the whole bay is mainly unaffected by the flood. Although the river discharges for the 1992 and 1999 flood are comparable, the transects in Fig. 9 show a different behaviour. Whereas in 1992 the bay has a nearly uniform salinity distribution, strong salinity stratifications are visible for 1999. These differences are mainly caused by the location of the strong rainfalls. For 1992, they occurred mostly in the southern parts of the Mary River catchments combined with minor precipitation in Hervey Bay. For 1999, the rainfalls were uniformly distributed over Hervey Bay and the catchments. Thus, due to the heavy precipitation, a freshening of the surface layer is visible (Fig. 9b) and explains the vertical salinity stratification. This is further explaining the greater width of the river plume. Both events are assisted by strong southerly winds. Hence, a northward flow-through in the Great Sandy Strait prevents an outflow of the Mary River discharge into the southern region of the Strait. This high flow-through further pushes the riverine water quite effectively into the bay. This is not the case for the 2008 floods. Due to the light winds, the fresh

Table 3: Atmospheric condition and river discharge for three flood events.

Year	River discharge	Wind direction	Wind speed
1992	7100 m^3/s	SE	6 m/s
1999	6700 m^3/s	S	8 m/s
2008	900 m^3/s	SE	3 m/s

water remains in the northern part of the Strait. Moreover, the saline water in the bay acts as a barrier, which prevents the transport of the riverine fresh water into Hervey Bay. Further, the low river discharge leads only to an weak coastal plume on the western shore (Fig. 9c).

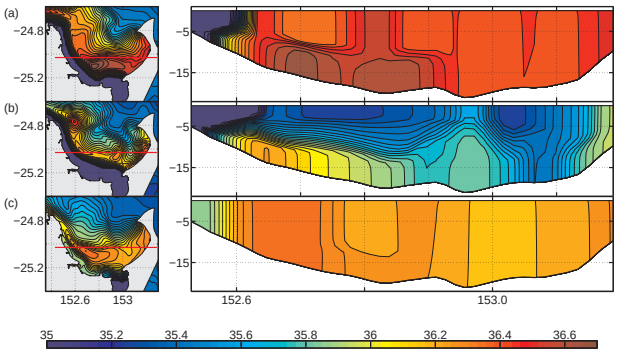

Figure 9: Depth averaged salinity (in psu) for a) 4 Mar. 1992, b) 20 Feb. 1999 and c) 23 Mar. 2008. In the left column the salinity transects along the red lines are shown. For visualisation, salinity values below 35 psu are set to 35 psu.

5.3. The flood of 1999

In the following, the 1999 flood event (February 1999) (Campbell and McKenzie, 2004) is used to estimate typical exchange time scales associated with high riverine flow, and also a time which is needed for Hervey Bay to recover to a "normal" state.

Two experiments are conducted. In the first one, called the flood run (FR), the river discharge, atmospheric boundary conditions and open ocean boundary conditions are prescribed using the forcing given in Sec. 2.2. At the same time, a neutral tracer with a concentration of 100 units was released into the river. In the second experiment, the control run (CR), the high river discharge due to the flood is completely switched off. Both experiments start at the 1. February 1999 and run for three months. Fig. 10 shows

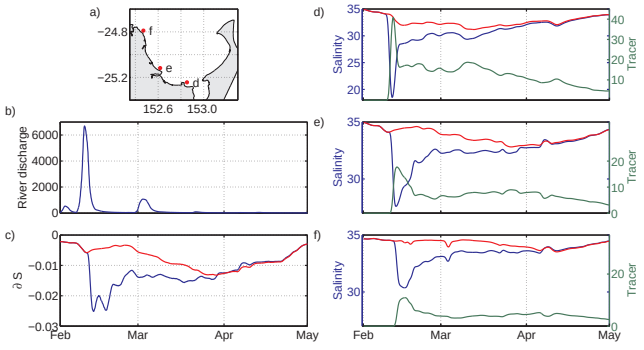

Figure 10: a) position of three virtual measurement stations to showing the impact of the 1999 flood, b) river discharge in m^3/s, c) salinity gradient ∂S in psu/km (see also Fig. 6). The blue curve represents the flood run (FR) and the red curve the control run (CR). Pictures d-f shows the salinity at the three stations d-f. The green curve indicates the tracer concentration.

the impact of the 1999 flood event. The peak river discharge is approx. 7600 m^3/s at the beginning of February. In the beginning of March a second minor flood occurred with a peak flow of 800 m^3/s. In Fig. 10c the impact of the flood on the salinity gradient is visible. The transect is positioned close to station f. The minimum gradient has a delay of 6 days compared to the flood peak. This corresponds to a plume velocity of 10 cm/s. Taking the wind conditions for this event into account (Tab. 3), clearly shows, that the plume is advected along the western shore due to the wind induced currents, (Gräwe et al. 2008). Fig. 10c further indicates that, although the salinity gradient shows a significant dip, Hervey Bay completely recovers to the undisturbed state (CR) within two months.

Fig. 10 d-f depict the change in salinity and tracer concentrations at the three stations. A closer inspection of the time series yield, that the minimum in the salinity and the maximum in concentration appear simultaneously. Thus, both are advected with the same velocity. Moreover the further north the station is situated, the weaker the flood impact. This seems quite reasonable, because the freshwater plume is much longer exposed to entrainment and tidal mixing. Nevertheless, the salinity time series show the same recovery time of 2 months to the undisturbed state. To compute a second time scale, it is assumed that

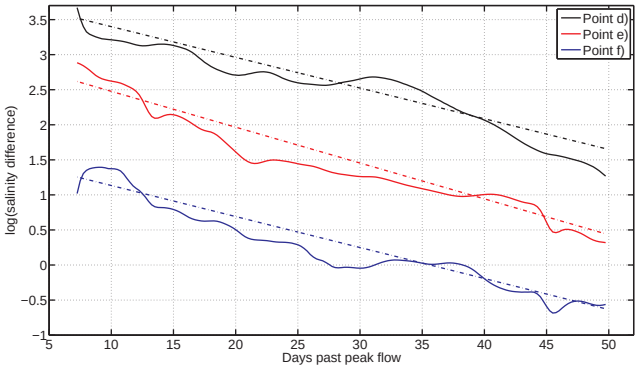

Figure 11: Time series of the logarithmic salinity difference (CR-FR) for the three virtual measurement stations (see Fig. 10a). The dashed lines indicate a linear fit. For visualisation, the time series are shifted along the y-axes

the salinity time series of exp. FR recovers exponentially to exp. CR. Fig. 11 depicts the logarithmic salinity difference between the exp. FR and exp. CR. The linear fits indicate that the exponential recovery is a reasonable assumption. Further, the exponential decay is nearly the same for all three stations. The linear fits indicate a decay constant of approx. 20-24 days. This time scale is similar to the flushing time of the western part of Hervey Bay under SE wind (Ribbe et al. 2008). Thus, the flushing of the riverine freshwater is strongly affected by wind conditions at the time.

5.4. Flood response

In the previous section a detailed analysis of the 1999 flood was given. The same exercise was repeated for the events of 1992 and 2008. In Tab. 4 the results are summarised. The simulation indicates, that although the flood related river discharges differs significantly, the recovery times vary only slightly. For all three events, Hervey Bay shows a decay rate of the disturbance, of approx. 22 days. This recovery time scale is seen in the salinity and in the salinity gradient time series. The simulations further indicate, that the flood response is closely related to the wind induced residual circulations.

Table 4: Exponential recovery time for the three flood events in days. The salinity recovery is averaged over the three stations. The salinity gradient ∂S is computed along the transect indicated in Fig. 2. For 2008, this measure could not be computed.

Year	River discharge	salinity recovery	∂S recovery
1992	7100 m^3/s	26 d	20 d
1999	6700 m^3/s	22 d	18 d
2008	900 m^3/s	20 d	-

6. Conclusion

The numerical modelling that was carried out made it possible to understand in detail, how the actual drying trend on the east coast of Australia impacted on the hydrodynamics of a coastal environment. This research was done for Hervey Bay, a subtropical coastal embayment that covers approx. 4000 km^2. Climatological data indicate that Hervey Bay exhibits features of an inverse/hypersaline estuary, due to the high evaporation rate of approximately 2 m/year and a low precipitation of less than 1 m/year. During the last two decades the drying trend has manifested in a reduction of precipitation by 13 % and a reduction in river discharge by 23 %. This is much higher than long-term variability suggested and shows the impact of severe droughts during the last two decades. As a direct consequence, hypersaline/inverse conditions are more persistent but they did not increase in magnitude. Further the baroclinic residual circulation accelerated by 18 % due to the disturbance of the evaporation/precipitation ratio. The signal visible in the salinity flux shows an increase by 22 %, however the annual variation are higher than the trend. Thus, longer simulation times should give more confidence, whether this is truly a trend or only long-term variations. Despite the drying trend, two major flood events occurred in Hervey Bay 1992 and 1999. The riverine freshwater flow is restricted to an approx. 10-15 km narrow band along the western shore of the bay. Essentially most of Hervey Bay is unaffected by the floods. The recovery time, to an undisturbed state, follows an exponential law with a typical decay time of 22 days. This time scale is similar to a flushing time for the western bay due to SE winds. Thus, the export of the freshwater is strongly affected by the wind conditions at the time of the event.
Due to the lack of validation data for biology/chemistry, only the impact on the hydrodynamics could be investigated. Therefore the understanding of the influence of the drying trend on the local flora/fauna would be of great interest but is at this stage of rather speculative nature.
Although the simulation time span is with 18 years rather short and is biased by severe El Niño/La Niña events, the simulations demonstrate that recent climate trends impacted on physical marine conditions in subtropical regions of eastern Australia and are likely to do so in the future if current climate trends, especially drying, are to continue.

Acknowledgement

We gratefully acknowledge the Bureau of Meteorology, Australia, Geoscience Australia and CSIRO Marine and Atmospheric Research for providing various data for this study. J. Ribbe would like the thank the Burnett Mary Regional Group for supporting the field program as well as the Hanse Institute for Advanced Study facilitating this collaboration.

References

[1] Beer, T., Borgas, M., Bouma, W., Fraser, P., Holper, P., Torok, S., 2006: Atmosphere. Theme commentary prepared for the 2006 Australia State of the Environment Committee, Department of Environment and Heritage, Canberra

[2] Bignami, F., Marullo, S., Santoleri, R., Schiano, M.E., 1995: Longwave radiation budget in the Mediterranean Sea, *Journal Geophysical Research*, 100(C2), 2501-2514

[3] Brink, K. H. and Shearman, R. K., 2006: Bottom boundary layer flow and salt injection from the continental shelf to slope, *Journal Geophysical Research Letter*, 33, L13608

[4] Campbell, S.J., McKenzie, L.J., 2004: Flood related loss and recovery of intertidal seagrass meadows in southern Queensland, Australia, *Estuarine, Coastal and Shelf Science*, 60, 477-490

[5] deCastro, M., Gomez-Gesteira, M., Alvarez, I., Prego, R., 2004: Negative estuarine circulation in the Ria of Pontevedra (NW Spain), *Estuarine, Coastal and Shelf Science*, 60, 301-312

[6] Fairall, C.W., Bradley, E.F., Hare, J.E., Grachev, A.A., Edson J.B., 2003: Bulk Parameterization of AirSea Fluxes: Updates and Verification for the COARE Algorithm, *Journal of Climate*, 16, 571-591

[7] Gräwe U., Wolff J.-O., Ribbe J., 2009, Mixing, Hypersalinity and Gradients in Hervey Bay, Australia, *Ocean Dynamics*, DOI: 10.1007/s10236-009-0195-4

[8] Growns, I., James, M., 2005: Relationships between river flows and recreational catches of Australian bass, *Journal of Fish Biology*, 66, 404

[9] Intergovernmental panel on climate change, IPCC, "Climate Change 2007", the Fourth IPCC Assessment Report, [http://www.ipcc.ch/ipccreports/]

[10] Ivanov, V.V., Shapiro, G. I., Huthnance, J. M., Aleynik, D. L., Golovin, P. N., 2004: Cascades of dense water around the world ocean, *Progress in Oceanography*, 60, 47-98

[11] Kennish, M.J., Livingston, R.J., Raffaelli, D., Reise, K., 2008: Environmental future of estuaries. In: N.V.C. Polunin (Ed.), Aquatic Ecosystems: Trends and Global Prospects, Cambridge University Press, Cambridge, pp. 188-208

[12] Labonne, M., Morize, E., Scolan, P., Lae, R., Dabas, E., Bohn, M., 2009: Impact of salinity on early life history traits of three estuarine fish species in Senegal, *Estuarine, Coastal and Shelf Science*, DOI: 10.1016/j.ecss.2009.03.005

[13] Largier, J.L., Hollibaugh, J.T., Smith, S.V., 1997: Seasonally hypersaline estuaries in Mediterranean-climate regions, *Estuarine, Coastal and Shelf Science*, 45, 789-797

[14] Lavin, M.R., Godinez, V.M., Alvarez, L.G., 1998: Inverse-estuarine Features of the Upper Gulf of California, *Estuarine, Coastal and Shelf Science*, 47, 769-795

[15] Lester, R.E., Fairweather, P.G., 2009: Modelling future conditions in the degraded semi-arid estuary of Australia's largest river using ecosystem states, *Estuarine, Coastal and Shelf Science*, DOI: 10.1016/j.ecss.2009.04.018

[16] Luyten, P. J., Jones, J. E., Proctor, R., Tabor, A., Tett, P., and Wild-Allen, K., 1999: COHERENS - A coupled hydrodynamical-ecological model for regional and shelf seas: user documentation, MUMM Rep., Management Unit of the Mathematical Models of the North Sea.

[17] Lyard, F., Lefevre, F., Letellier, T., Francis, O., 2004: Modelling the global ocean tides: modern insights from FES2004, *Ocean Dynamics*, 56, 394-415.

[18] Masoner, J.R., Stannard, D.I., Christenson S.C., 2008: Differences in evaporation between a floating pan and class A pan on land, *Journal of the American water resources association*, 44, 3

[19] Mellor, G.L., Yamada, T., 1982: Development of a turbulence closure model for geophysical fluid problems, *Review of Geophysical Space Physics*, 20, 851-875

[20] Meynecke, J.-O, Lee, S.Y., Duke, N.C., Warnken, J., 2006: Effect of rainfall as a component of climate change on estuarine fish production in Queensland, Australia, *Estuarine, Coastal and Shelf Science*, 69, 491-504

[21] Mikhailova, V.N., Isupovab, 2008: M.V., Hypersalinization of River Estuaries in West Africa, *Water Resources*, 35(4), 367-385

[22] Murphy, B.F., Ribbe, J. 2004: Variability of southeast Queensland rainfall and its predictors, *Int. Journal of Climatology*, 24(6), 703-721

[23] Nunes Vaz, R.A., Lennon, G.W., Bowers, D.G., 1990: Physical behaviour of a large, negative or inverse estuary, *Continental Shelf Research*, 10, 277-304

[24] Oke, P.R., Middleton, J.H., 1999: Topographically Induced Upwelling off Eastern Australia, *Journal of Physical Oceanography*, 30, 512-531

[25] Preen, A.R., Lee Long, W.J., Coles, R.G., 1995: Flood and cyclone related loss, and partial recovery, of more the 1000 km^2 of seagrasses in Hervey Bay, Queensland, Australia, *Aquatic Botany* 52, 3-17

[26] Rayment, G.E., Neil, D., 1997: Sources of material in river discharge, *The Great Barrier Reef: Science, Use and Management, James Cook University, Townsville*, 1, 42-59

[27] Ribbe, J., 2006: A study into the export of saline water from Hervey Bay, Australia, *Estuarine, Coastal and Shelf Science*, 66, 550-558

[28] Ribbe, J., Wolff, J.-O., Staneva, J., Gräwe, U., 2008: Assessing Water Renewal Time Scales for Marine Environments from Three-Dimensional Modelling: A Case Study for Hervey Bay, Australia, *Environmental Modelling and Software*, 3, 1217-1228

[29] Ribbe, J., 2008: Monitoring and Assessing Salinity and Temperature Variations in Hervey Bay. Final Report prepared for the Burnett Mary Regional Group, Bundaberg, Australia, http://www.usq.edu.au/users/ribbe/

[30] Ridgway, K.R., Godfrey, J. S., 1997: Seasonal cycle of the East Australian Current, *Journal Geophysical Research*, 102, 22921-22936

[31] Saunders, P., Coward, A.C., de Cuevas, B.A., 1999: Circulation of the Pacific Ocean seen in a global ocean model: Ocean Circulation and Climate Advanced Modelling project (OCCAM), *Journal Geophysical Research*, 104, 18281-18299

[32] Schaffelke, B, 2002: A review of water quality issues influencing the habitat quality in dugong protection areas, *Great Barrier Reef Marine Park Authority, Research Publication*, 66-78

[33] Seidel, D. J., Fu, Q., Randel, W. J., and Reichler, T. J., 2008: Widening of the tropical belt in a changing climate, *Nature Geoscience*, 1, 21-24.

[34] Shi, G., Cai, W., Cowan, T., Ribbe, J., Rotstayn, L., Dix, M., 2008a: Variability and trend of the northwest Western Australia Rainfall: observations and coupled climate modelling, *Journal of Climate*, 21, 2938-2959

[35] Shi, G., Ribbe, J., Cai, W., Cowan, T. 2008b: Interpretation of Australian summer and winter rainfall projections, *Journal Geophysical Research Letter*, 35, L02702

[36] Staunton-Smith, J., Robins, J.B., Mayer, D.G., Sellin, M.J., Halliday, I.A., 2004: Does the quantity and timing of fresh water flowing into a dry tropical estuary affect year-class strength of barramundi (Lates calcarifer)? *Marine and Freshwater Research*, 55, 787-797

[37] Tanny, J., Cohen, S., Assouline, S., Lange, F., Grava, A., Berger, D., Teltch, B., Parlange, M.B., 2008: Evaporation from a small water reservoir: Direct measurements and estimates, *Journal of Hydrology*, 351, 218 229

[38] Tomczak, M. and Godfrey, S., 2003: Regional Oceanography: an Introduction. 2nd edition. *Daya Publishing House*, Delhi, 390 pp

[39] Ward, T.M., Staunton-Smith, J., Hoyle, S., Halliday, I.A., 2003: Spawning patterns of four species of predominantly temperate pelagic fishes in the subtropical waters of southern Queensland, *Estuarine, Coastal Shelf Science*, 56, 1125-1140

[40] Wolanski E., 1986: An evaporation-driven salinity maximum zone in Australian tropical estuaries, *Estuarine, Coastal Shelf Science*, 22, 415-424